

# Thermally accessible triplet state of $\pi$ -nucleophiles does exist. Evidence from first principles study of ethylene interaction with copper species

Sergey V. Bondarchuk<sup>\*a</sup> and Boris F. Minaev<sup>a,b</sup>

---

<sup>a</sup> Department of Organic Chemistry, Bogdan Khmelnitsky Cherkasy National University, blvd. Shevchenko 81, 18031 Cherkasy, Ukraine. Fax: (+3) 80472 37-21-42; Tel: (+3) 80472 37-65-76;

E-mail: bondchem@cdu.edu.ua

<sup>b</sup> Department of Theoretical Chemistry and Biochemistry, Royal Institute of Technology, AlbaNova, S-106 91 Stockholm, Sweden

## SUPPORTING INFORMATION

*RSC Advances*

**LIST OF SUPPLEMENTARY FIGURES AND TABLES:**

<b>Figure S1.</b> Six possible adsorption sites of ethylene on the Cu(100) surface.....	3
<b>Figure S2.</b> Bond critical points, which are found in the supercell content.....	3
<b>Figure S3.</b> Electronic band structure (left) and partial density of states (right) plots of clean Cu(100) surface (top) and covered by ethylene (bottom).....	4
<b>Figure S4.</b> Structures of the odd-numbered copper clusters optimized by the DFT(UM06)/LANL2DZ method in ethanol medium. Blue labels correspond to the point group symmetry.....	5
<b>Figure S5.</b> Correlation of different parameters with the number of copper atoms $n$ : a) the SOMO-LUMO gap; b) spin density on the reacting copper atom; c) vibrational frequencies of the band I and II; d) the C=C Laplacian bond order and the $\pi\sigma$ parameter.....	6
<b>Table S1.</b> The single-occupied (SOMO) and the lowest unoccupied (LUMO) molecular orbital energies of the calculated copper clusters; $\Delta E$ is the SOMO-LUMO energy gap.....	6
<b>Table S2.</b> Coordination numbers and free valence values of the carbon atoms in the $C_2H_4/Cu_n$ complexes.....	7
<b>Figure S6.</b> Selected structural and QTAIM topological parameters of the $C_2H_4/Cu^+$ and $C_2H_4/Cu^{2+}$ complexes. Pink circles indicate the bond critical points between the ethylene moieties and copper ion.....	7
<b>Figure S7.</b> Calculated IR spectra of the $C_2H_4/Cu$ complex in the $\tilde{X}^2A'$ (blue) and ${}^2B_2$ (red) states. The band I and II are indicated by vertical arrows.....	8
<b>Figure S8.</b> Calculated UV-vis spectra of the $C_2H_4/Cu$ complex in the $\tilde{X}^2A'$ (blue) and ${}^2B_2$ (red) states.....	8
<b>Table S3.</b> Performance of different functionals in prediction of the two experimentally observed bands in the UV-vis spectrum of the $C_2H_4/Cu$ complex ( $\tilde{X}^2A'$ state).....	8
<b>Figure S9.</b> Energies of frontier molecular orbitals of the $C_2H_4/Cu$ complex ( ${}^2B_2$ state) as function of the C–Cu interatomic distance.....	9
<b>Figure S10.</b> The QST3-optimized transition state structure and the related minima (top); the corresponding IRC path (bottom).....	10

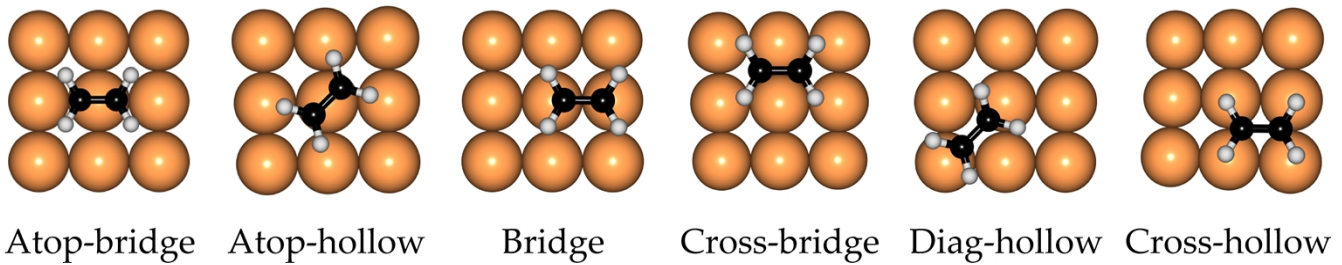


**Figure S1.** Six possible adsorption sites of ethylene on Cu(100) surface.

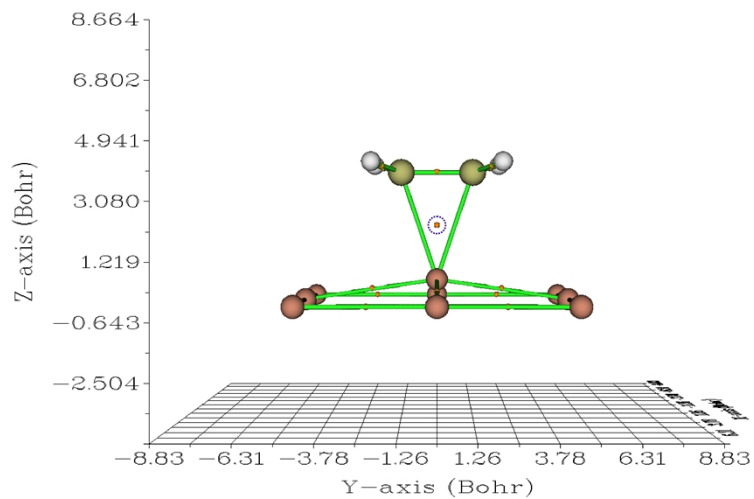


**Figure S2.** Bond critical points, which are found in the supercell content.

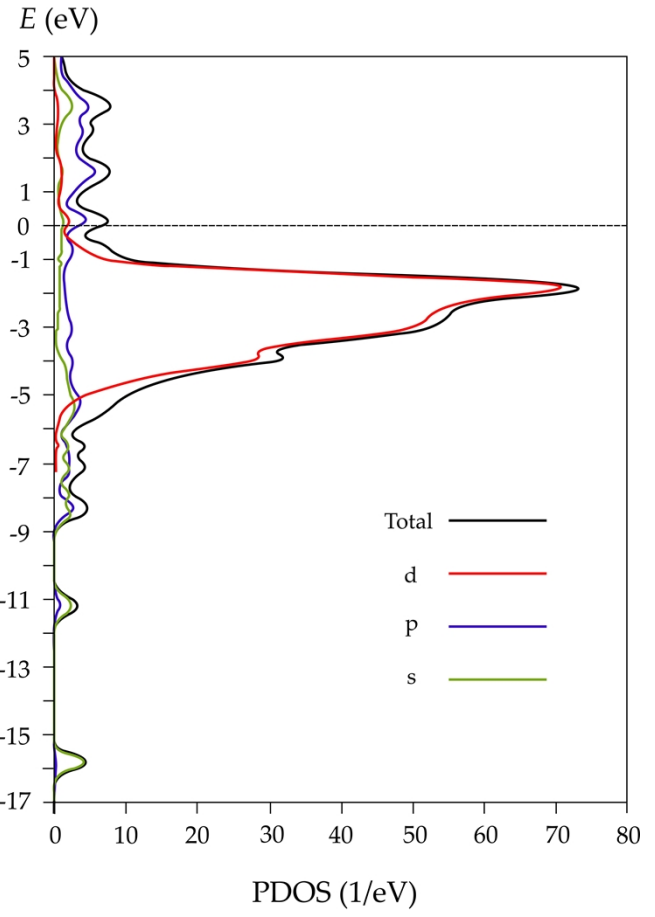
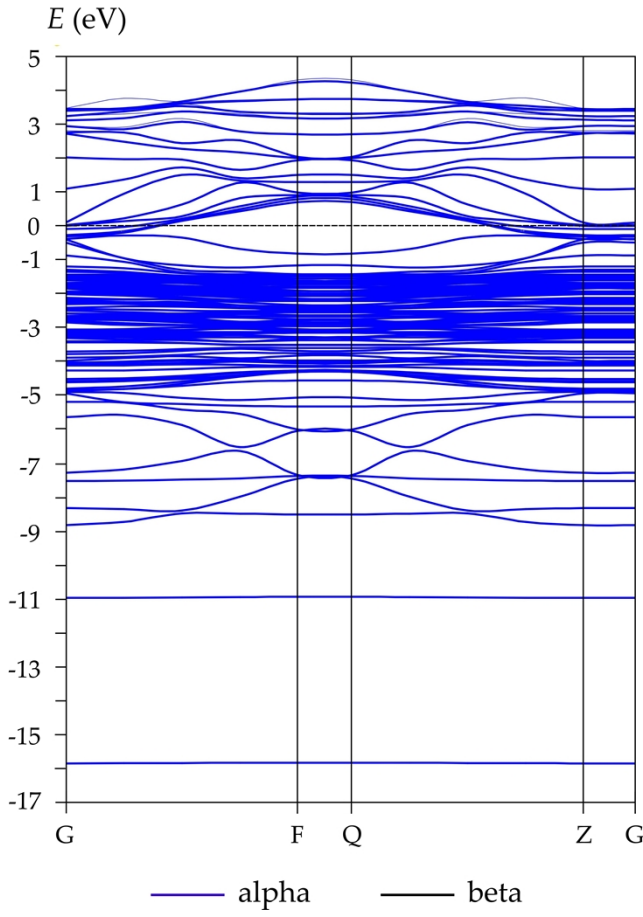
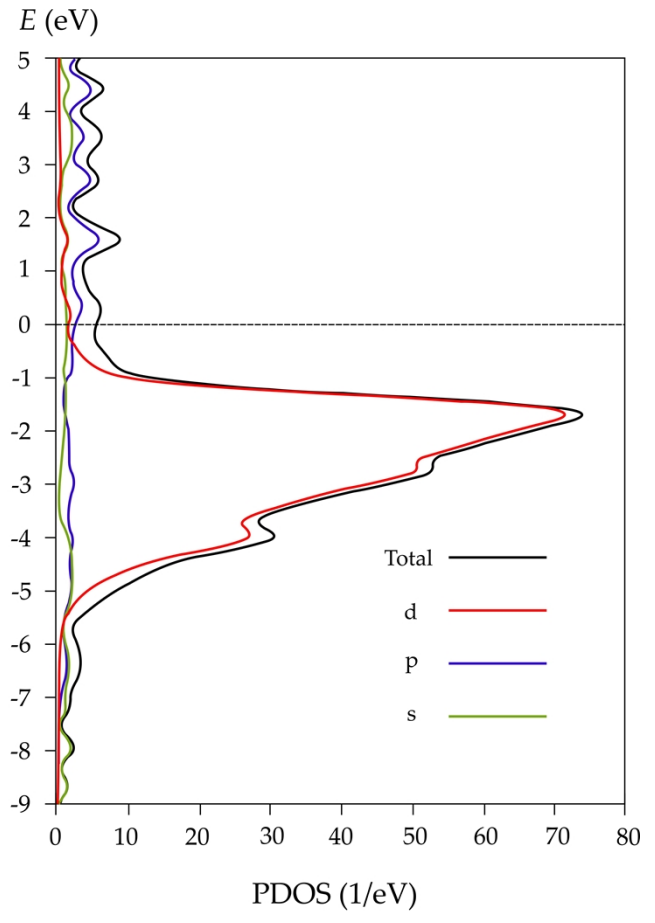
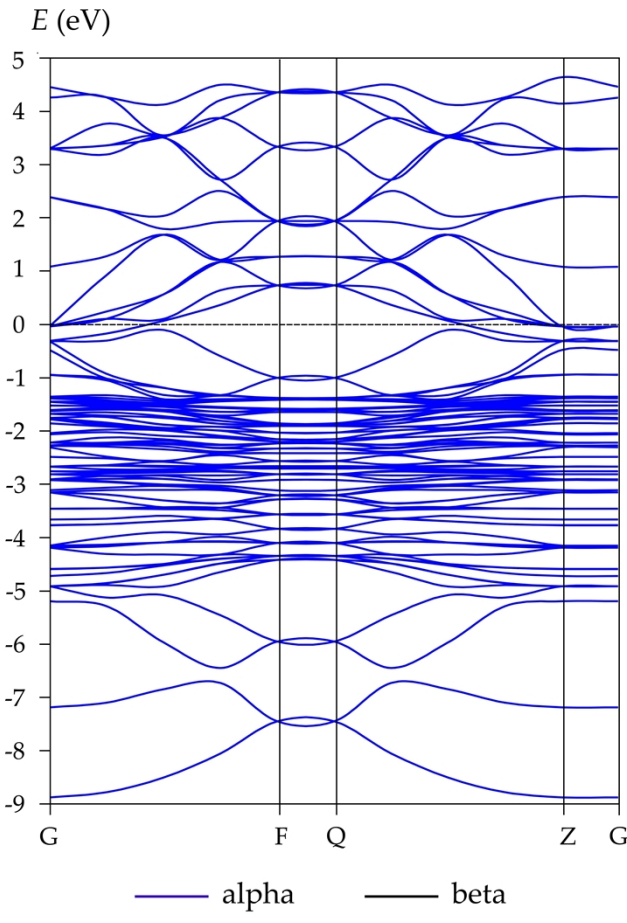


**Figure S3.** Electronic band structure (left) and partial density of states (right) plots of clean Cu(100) surface (top) and covered by ethylene (bottom).

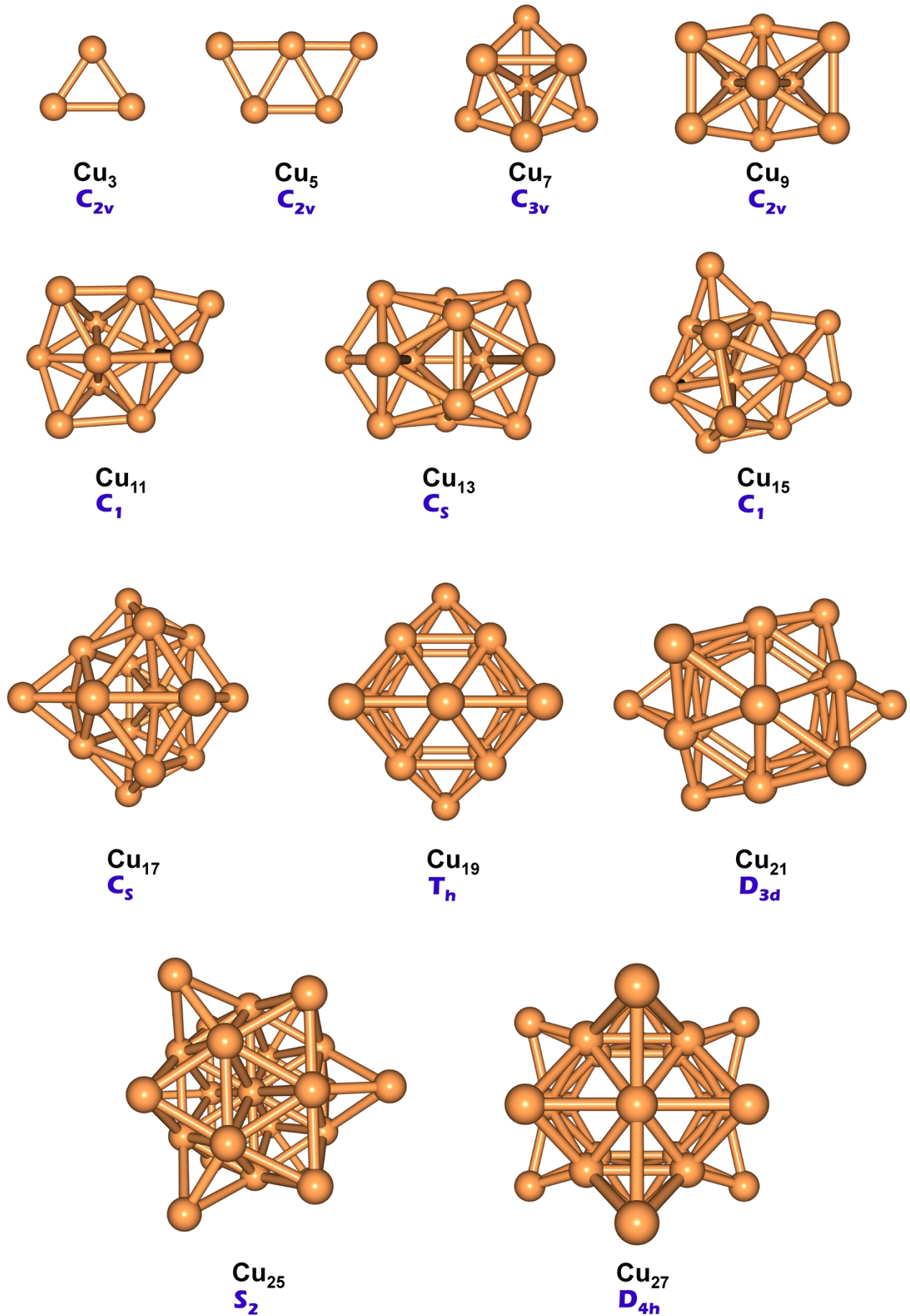


**Figure S4.** Structures of the odd-numbered copper clusters optimized by the DFT(UM06)/LANL2DZ method in ethanol medium. Blue labels correspond to the point group symmetry.

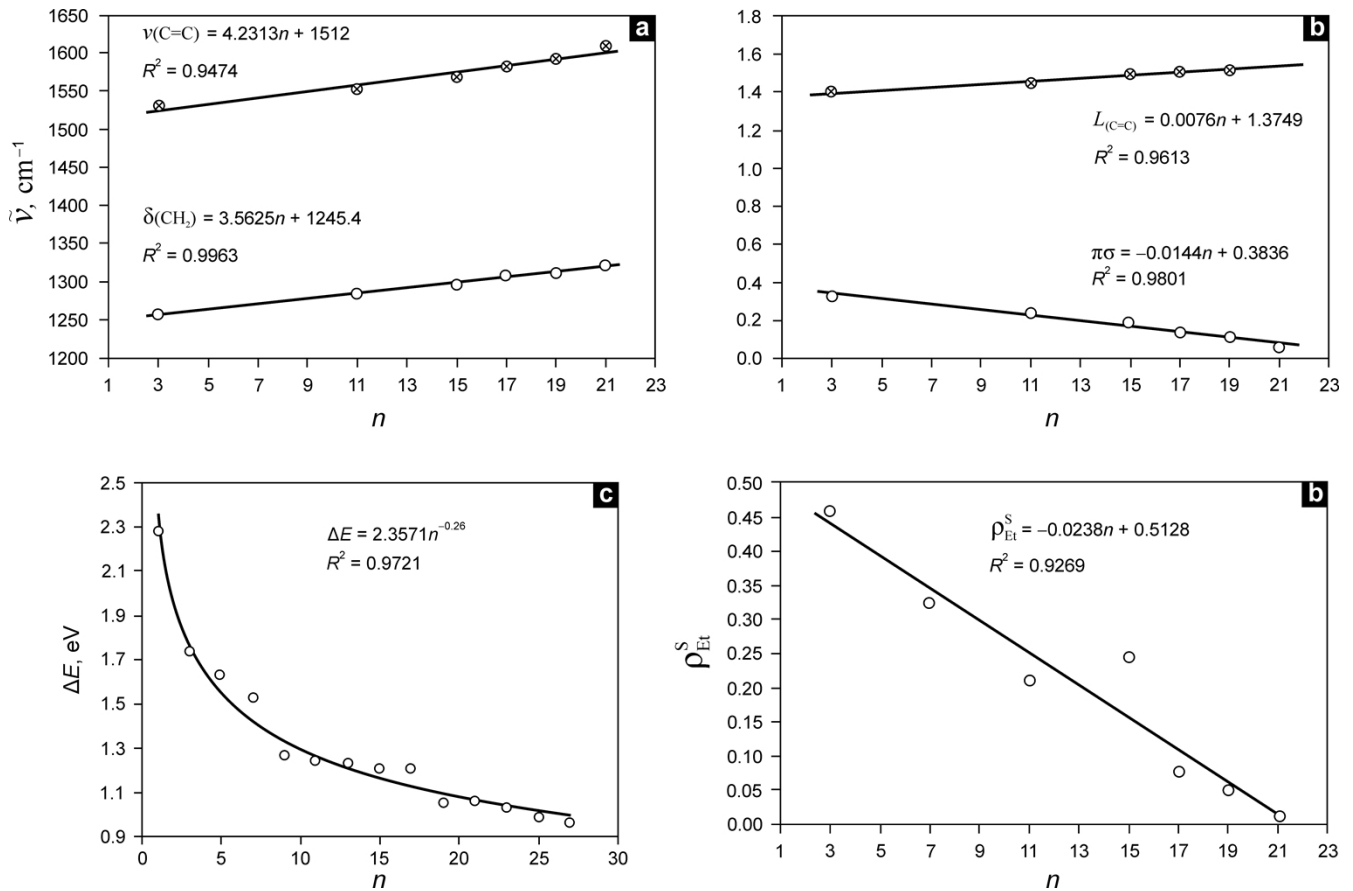


**Figure S5.** Correlation of different parameters with the number of copper atoms  $n$ : a) vibrational frequencies of the band I and II; b) the C=C Laplacian bond order and the  $\pi\sigma$  parameter; c) the SOMO-LUMO gap; d) spin density on the reacting copper atom.

**Table S1.** The SOMO and the LUMO energies of the calculated copper clusters;  $\Delta E$  is the SOMO-LUMO energy gap.

$n$	$E_{\text{SOMO}}$ , eV	$E_{\text{LUMO}}$ , eV	$\Delta E$ , eV
1	-5.03	-2.75	2.28
3	-3.87	-2.13	1.74
5	-4.50	-2.88	1.63
7	-4.56	-3.03	1.53
9	-3.81	-2.54	1.27
11	-4.10	-2.85	1.25
13	-4.15	-2.91	1.23
15	-4.23	-3.02	1.21
17	-4.67	-3.46	1.21
19	-4.52	-3.47	1.05
21	-4.56	-3.49	1.06
23	-3.98	-2.94	1.04
25	-4.31	-3.32	0.98
27	-4.19	-3.23	0.96

**Table S2.** Coordination numbers and free valence values of the carbon atoms in the C<sub>2</sub>H<sub>4</sub>/Cu<sub>n</sub> complexes.

n	Coordination number <sup>a</sup>		Free valence <sup>b</sup>	
	C1	C2	C1	C2
3	3.9490	3.9490	0.0022	0.0020
7	3.9320	3.9330	0.0055	0.0054
11	3.9822	3.9612	0.0015	0.0029
15	3.9281	3.9189	0.0008	0.0007
17	3.9170	3.9047	0.0002	0.0003
19	3.9244	3.9244	0.0010	0.0010
21	3.9042	3.9051	0.0021	0.0016

<sup>a</sup> Calculated as the following:<sup>S1</sup>

$$CN_A = \sum_B \frac{1}{1 + \exp\left(-16 \cdot ((4/3)(R_A + R_B)/r - 1)\right)}$$

Herein R is covalent radius taken from Ref. S2.

<sup>b</sup> Calculated as the following:<sup>S3</sup>

$$F_A = V_A - \sum_{B \neq A} B_{AB} = \sum_{\mu, \nu} (\mathbf{P}^S \mathbf{S}^A)_{\mu \nu} (\mathbf{P}^S \mathbf{S}^A)_{\nu \mu}$$

where  $\mathbf{P}^S$  is the spin density;  $V_A$  is the total valence of atom A and is calculated according to the following equation:

$$V_A = 2Q_A - \sum_{\mu, \nu} (\mathbf{D} \mathbf{S}^A)_{\mu \nu} (\mathbf{D} \mathbf{S}^A)_{\nu \mu}$$

Herein  $Q_A$  is Hirshfeld's atomic population;  $\mathbf{D}$  is total density.<sup>S3</sup>

<sup>S1</sup>Grimme, S.; Antony, J.; Ehrlich, S.; Krieg, H. A Consistent and Accurate ab initio Parametrization of Density Functional Dispersion Correction (DFT-D) for the 94 Elements H–Pu. *J. Chem. Phys.* **2010**, *132*, 154104.

<sup>S2</sup>Pyykkö, P.; Atsumi, M. Molecular Single-Bond Covalent Radii for Elements 1–118. *Chem.—Eur. J.* **2008**, *15*, 186–197.

<sup>S3</sup>Mayer, I.; Salvador, P. Overlap Populations, Bond Orders and Valences for “Fuzzy” Atoms. *Chem. Phys. Lett.* **2004**, *383*, 368–375.

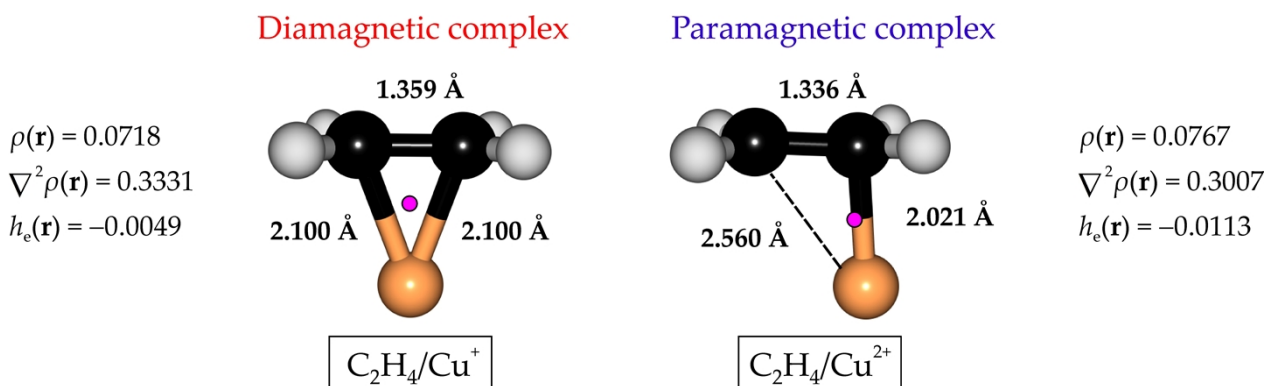


**Figure S6.** Selected structural and QTAIM topological parameters of the C<sub>2</sub>H<sub>4</sub>/Cu<sup>+</sup> and C<sub>2</sub>H<sub>4</sub>/Cu<sup>2+</sup> complexes. Magenta circles indicate the bond critical points between the ethylene moieties and the copper ion.

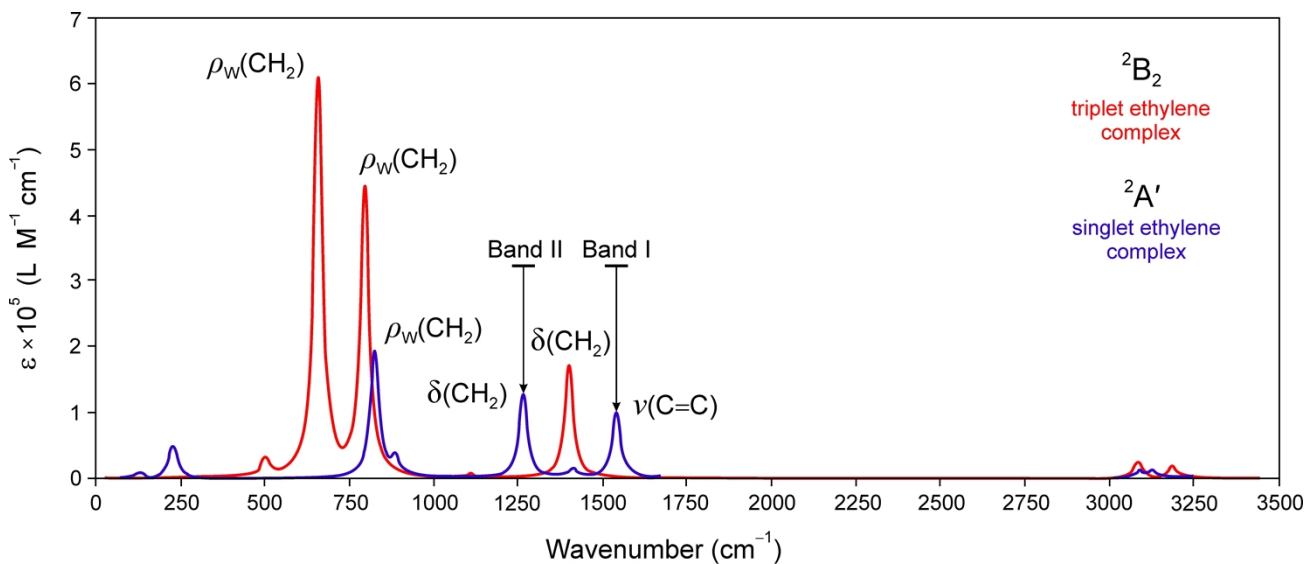


**Figure S7.** Calculated IR spectra of the  $\text{C}_2\text{H}_4/\text{Cu}$  complex in the  $\tilde{\chi}^2\text{A}'$  (blue) and  ${}^2\text{B}_2$  (red) states. The band I and II are indicated by vertical arrows.

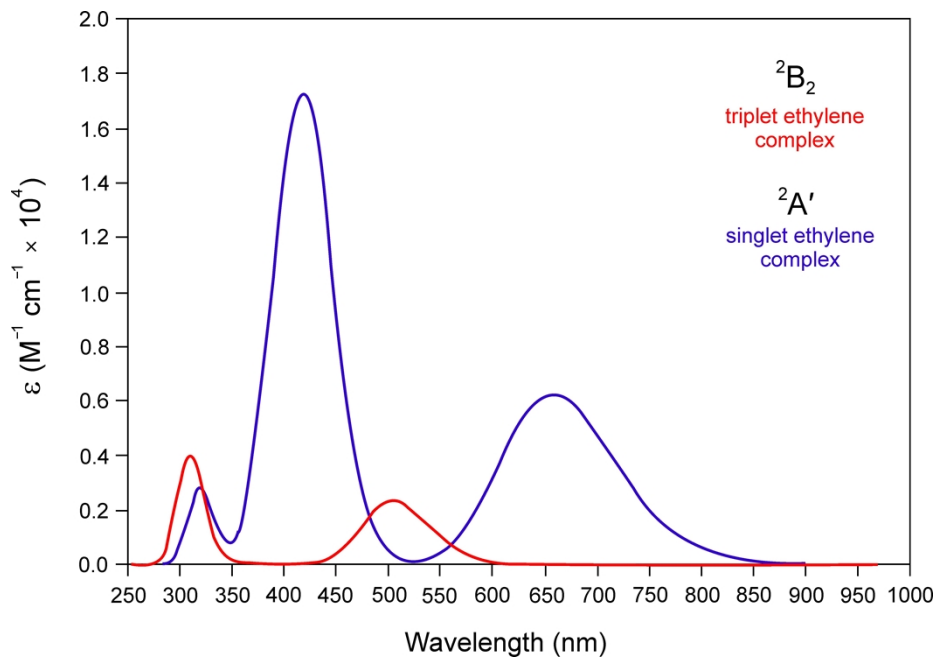


**Figure S8.** Calculated UV-vis spectra of the  $\text{C}_2\text{H}_4/\text{Cu}$  complex in the  $\tilde{\chi}^2\text{A}'$  (blue) and  ${}^2\text{B}_2$  (red) states.

**Table S3.** Performance of different functionals in prediction of the two experimentally observed bands in the UV-vis spectrum of the  $\text{C}_2\text{H}_4/\text{Cu}$  complex ( $\tilde{\chi}^2\text{A}'$  state).

M062X	BMK	B3LYP	PBE0	HSE06	$\omega$ B97XD	B97D	mPW1PW91	BH&HLYP	CAM-B3LYP
441	392	398	412	405	415	394	408	424	398
344	313	338	333	331	323	—	331	337	319

## Mixing SOMO and LUMO

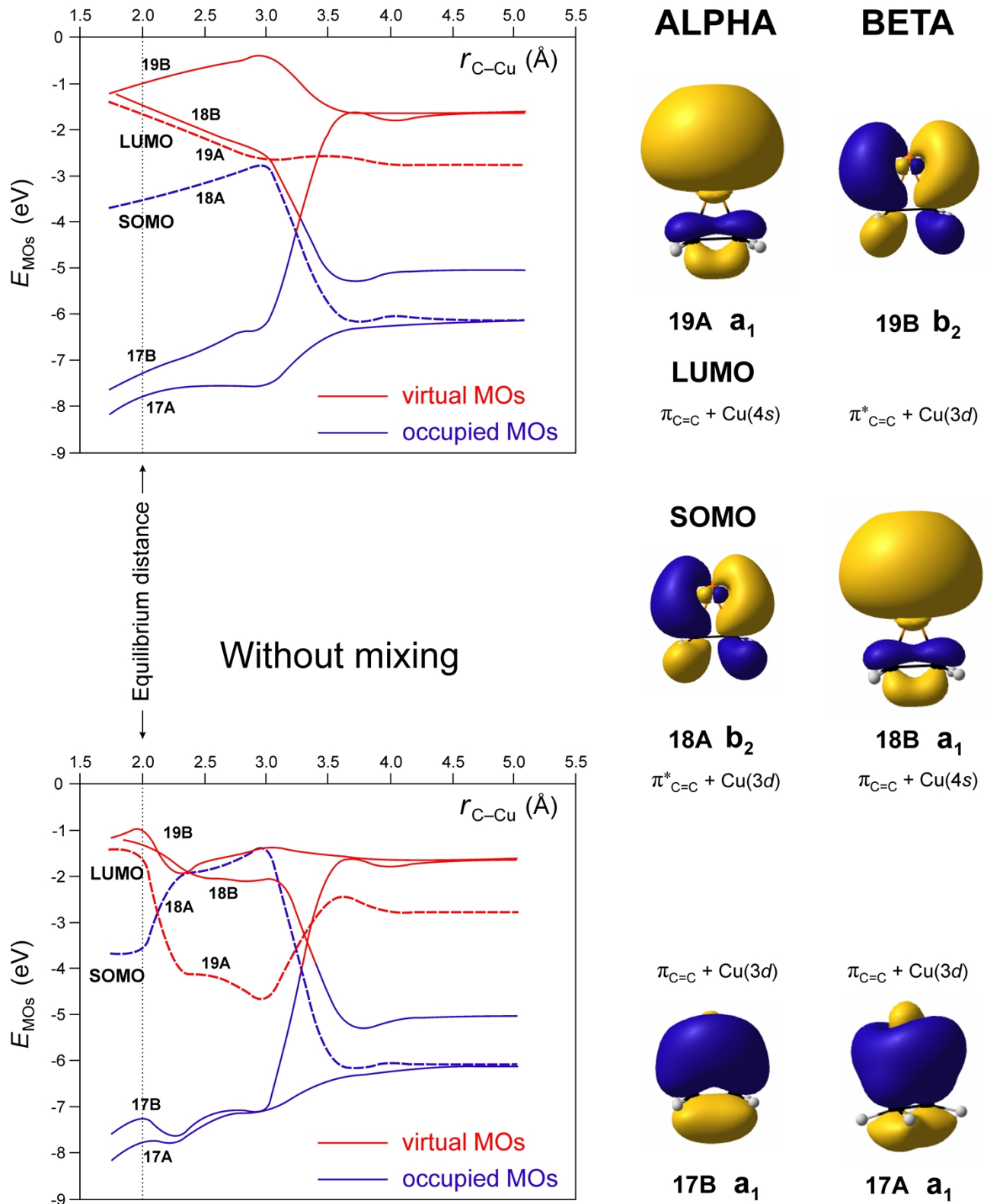


**Figure S9.** Energies of frontier molecular orbitals of the  $C_2H_4/Cu$  complex ( ${}^2B_2$  state) as function of the C–Cu interatomic distance.

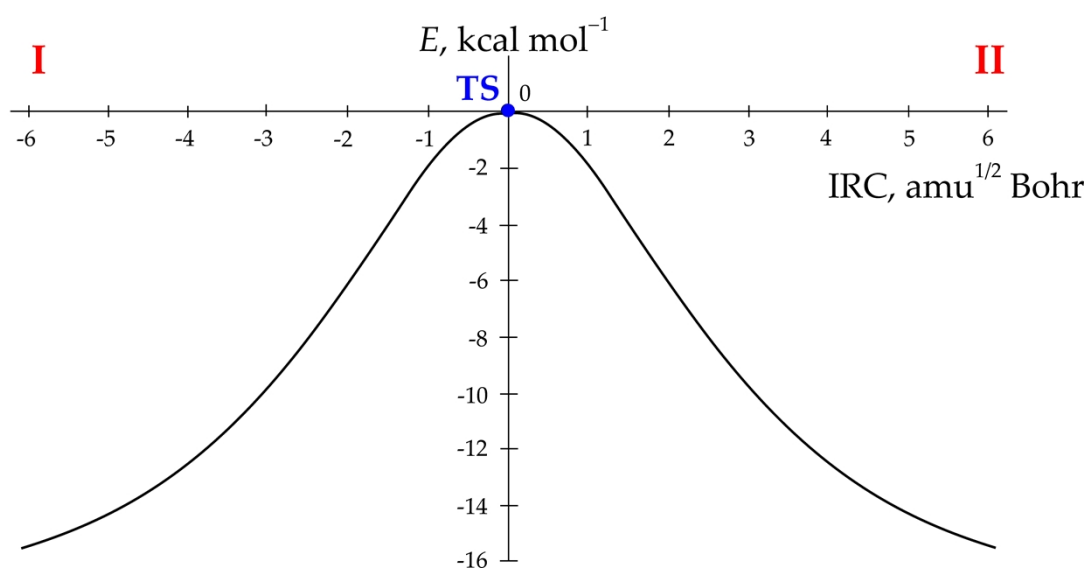
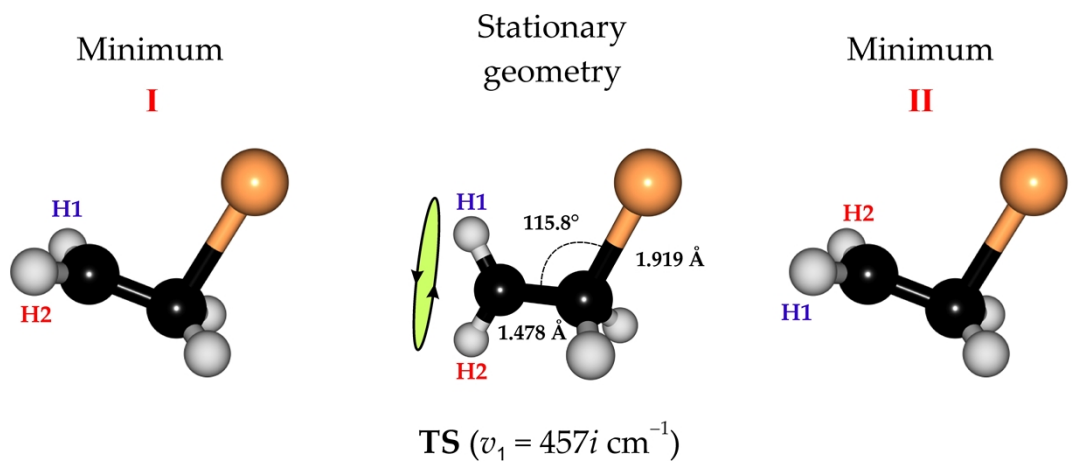


**Figure S10.** The QST3-optimized transition state structure and the related minima (top); the corresponding IRC path (bottom).